RSC Advances

PAPER

View Article Online
View Journal | View Issue

Cite this: *RSC Adv.*, 2026, **16**, 19895

Precipitation of vanadium from leachate solutions by reduction with hydrazine

Aston C. Pearcy, [ac] Brooke L. Matthews, [ac] Aaron T. Marshall [bc] and Chris W. Bumby *[ac]

Vanadium is a 'critical metal' with wide reaching applications. Current methods to extract vanadium from ores and slags rely on generating a solution of pentavalent vanadium ions, which are then precipitated using ammonium salts to form a vanadium-bearing solid. However, this precipitation method generates large volumes of unrecyclable wastewater which must be discharged. Herein, we describe a cleaner method to precipitate vanadium from leachate solutions, by reduction with dilute aqueous solutions of hydrazine. This approach generates a nano-colloidal suspension that can be agglomerated to give precipitation efficiencies of up to 94%, and product purities of up to 99.5%. This is a zero-liquid-discharge method – after reduction, hydrazine is oxidised to volatile by-products which can be removed by simply heating. Therefore, this process outputs only solid material, whilst retaining all liquids within a closed-loop process.

Received 2nd April 2026
Accepted 2nd April 2026

DOI: 10.1039/d6ra02758j

rsc.li/rsc-advances

Introduction

Vanadium is a 'critical metal', with applications in high-strength steel and other specialist alloys,[1,2] and as a catalyst in the production of sulfuric acid and maleic anhydride.[3,4] An emerging use of vanadium is as an electrolyte in vanadium redox flow batteries (VRFB),[5,6] a promising technology for long-term energy storage. Demand from these applications, particularly from the VRFB industry, is continually growing.[7]

Vanadium is widely dispersed in nature, typically occurring at low concentrations.[8] Approximately ~70% of the world's vanadium is produced as a by-product of primary processes,[9] notably steelmaking, where vanadium is recovered from steel slags generated during smelting.[10] A minor amount of the world's vanadium supply is extracted directly from vanadium-bearing titano-magnetite ores.[11]

Vanadium is commonly extracted from slags or ores using hydrometallurgical processes.[12,13] These processes typically include oxidative roasting, aqueous leaching, and precipitation steps. The conventional industrial method comprises sodium-roasting, followed by water-leaching and ammonium-salt precipitation (Fig. 1).[14–19] This approach has significant environmental drawbacks. Firstly, the roasting step produces corrosive gases such as Cl_2 and SO_2;[20,21] secondly, the leaching step solubilises toxic hexavalent chromium, a known carcinogen;[22] and, thirdly, the precipitation step leaves behind a large amount of unrecyclable saline ammonia wastewater, which is contaminated extensively with non-volatile salts and must be discharged (red box Fig. 1).[23,24] Increasingly strict environmental regulations around wastewater handling and growing public awareness surrounding industry practice is

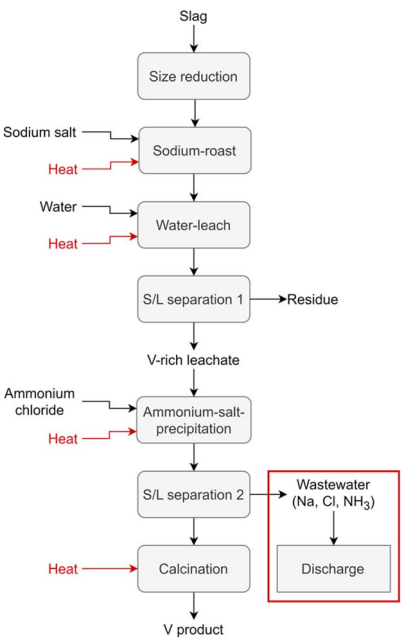

Fig. 1 Process flow diagram of the conventional sodium-roast water-leach ammonium-salt-precipitation route.

[a]*Robinson Research Institute, Victoria University of Wellington, Lower Hutt, New Zealand. E-mail: chris.bumby@vuw.ac.nz*

[b]*Department of Chemical and Process Engineering, University of Canterbury, Christchurch, New Zealand*

[c]*The MacDiarmid Institute for Advanced Materials and Nanotechnology, Victoria University of Wellington, Wellington, New Zealand*

encouraging a shift to greener technologies for vanadium extraction,[25–31] such as zero-liquid-discharge methods.[32]

Alternative roasting and leaching methods have been proposed.[25,26,33] However, most efforts to improve the precipitation step involve modifications or upgrades to the existing ammonium-salt method.[34–37] Ammonium-salt precipitation leaves behind soluble by-products (*e.g.* salts) in solution which are difficult to remove, inhibiting recycling of the leachate solution and resulting in the discharge of contaminated wastewater. While literature work has, to some extent, improved the ammonium-salt process,[37–39] the underlying problems of excess reagent consumption and production of large volumes of unrecyclable hazardous wastewater remain unresolved. Therefore, there is a critical need for a new, cleaner precipitation method.

Vanadium can exist in multiple oxidation states (V^{2+}, V^{3+}, V^{4+}, and V^{5+}), which have varying solubility in aqueous solution. In vanadium-bearing ores and slags, vanadium predominantly occurs as the insoluble V^{3+} ion. To enable leaching, the slag is oxidised using an oxidatively roasting step, which generates the more soluble V^{5+} ion.[40,41] This allows the vanadium to be leached and affords a solution containing vanadium complexes in which vanadium is in the V^{5+} oxidation state (highlighted yellow region Fig. 2). The difference in aqueous solubility between oxidation states of vanadium could be used in a precipitation process, whereby V^{5+} ions are reduced to lower oxidation states that are less soluble. This can be conceptualised as travelling down the E_H axis on the vanadium Pourbaix diagram in water (green arrow Fig. 2), as opposed to the conventional reactive precipitation method with ammonium salts, which moves across the pH axis (red arrow Fig. 2).

Hydrazine hydrate is a potential reductant for vanadium precipitation. Although widely used in organic and inorganic synthesis procedures,[42–45] its application in hydrometallurgical processes remains relatively unexplored. Its liquid state at ambient temperature facilitates handling, storage, and controlled introduction into a reaction. Upon reduction, hydrazine is oxidised to volatile by-products (eqn (1) and (2)), which can be readily separated from reaction media *via* the gas-phase by heating or reducing pressure. This clean decomposition prevents contamination of the process stream and could enable full recycling of the leachate solution.

$$N_2H_4 + xM^{n+} \rightarrow xM^{(n-4/x)+} + N_2\uparrow + 2H_2\uparrow \quad (1)$$

$$2N_2H_4 + xM^{n+} \rightarrow xM^{(n-2/x)+} + N_2\uparrow + 2NH_3\uparrow + H_2\uparrow \quad (2)$$

An emerging improvement to the roasting and leaching steps is the use of a non-salt air roast followed by ammonium bicarbonate leaching. Recent studies report that a non-salt air roast ammonium bicarbonate-leach process has high leaching efficiency and selectivity for vanadium,[25,26] whilst being cleaner than other methods, such as the conventional sodium-roast water-leach. Ammonium bicarbonate decomposes upon heating to volatile gaseous species, which can be removed and recirculated into a closed-loop system. Furthermore, vanadium species produced by blank-roasting are soluble in ammonium bicarbonate, eliminating the need for additives in the roast—a requirement when water is used as the lixiviant in the conventional method—thereby reducing reagent usage and eliminating the generation of persistent wastewater. Due to these advantages, ammonium bicarbonate was utilised as a clean lixiviant in our hydrazine precipitation process.

A process flow diagram of the proposed zero-liquid-discharge route based on hydrazine precipitation is shown in Fig. 3. The deliberately designed reagent system produces exclusively volatile by-products, which are easily removed from the lixiviant solution. Consequently, after precipitation, the

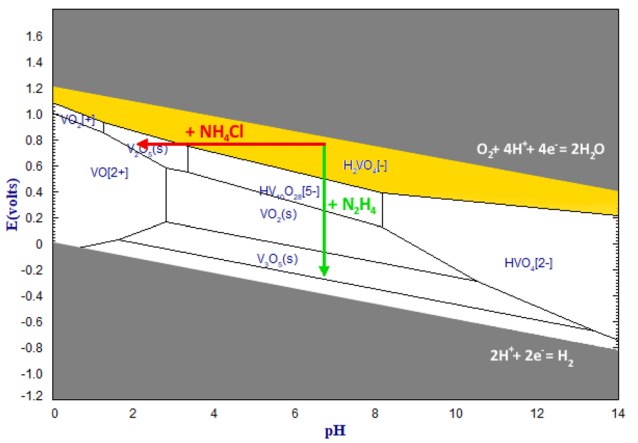

Fig. 2 FactSage calculated Pourbaix diagram of the V–O–H system at 298.15 K. Soluble V concentration set to 10 mmol L^{-1}. Green arrow represents the proposed hydrazine precipitation process, red arrow represents the conventional ammonium-salt precipitation method with ammonium chloride.

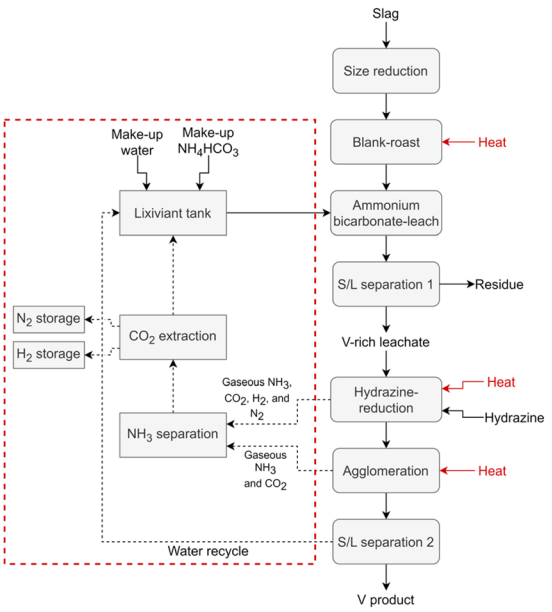

Fig. 3 Proposed process flow diagram for the zero-liquid-discharge process created from the combination of ammonium bicarbonate leaching and hydrazine precipitation. Note that operations in the red dotted box have not been demonstrated in this work.

leftover leachate can be recycled back to the leaching step, eliminating wastewater discharge.

In this study, we use aqueous solutions of hydrazine hydrate to precipitate vanadium-bearing solids from leachate solutions produced through ammonium bicarbonate leaching of slags. We then examine the composition and morphology of these precipitates and show that this hydrazine precipitation is cleaner than the dominant industrial method.

Experimental

Materials and methods

Vanadium-bearing slags (Vanadium Recovery Concentrate (VRC) and Alkaline Converter (AC) slags) were obtained from New Zealand Steel (Glenbrook) and used as received. Unless specified, all other chemicals were of analytical grade and were obtained from commercial sources. Aqueous 15% ammonium bicarbonate lixiviant solution was made by dissolving 150 g of ammonium bicarbonate in 1 L distilled water. X-ray diffraction (XRD) analysis was conducted using a Bruker D8 Advance diffractometer with Co-Kα radiation. X-ray fluorescence (XRF) measurements were conducted on a Shimadzu EDX-7200 Energy Dispersive X-ray fluorescence spectrometer. Transmission Electron Microscopy (TEM) imaging was conducted on a JEOL JEM-2100F machine with an accelerating voltage of 200 kV. Samples for TEM were dispersed in either water or ethanol and the dispersion was dropped directly onto a copper grid. Zeta potential measurements and particle size analysis of colloidal solutions were conducted on a Zetasizer Nano (2009 model), using distilled water that was filtered twice through a 0.45 μm nylon membrane as the dispersant.

Slag compositions

The compositions of the slags used in this study were analysed *via* XRF and are shown below (Table 1).

Preparation of leachate solutions from vanadium-bearing slags

AC leachate. AC slag was milled in a ring mill for 30 seconds, and then roasted in a muffle furnace for 1 h at 1000 °C. This roasted material was ground in a ring mill for 5 seconds. The powder was then added to 15% ammonium bicarbonate solution at an 8.33 : 1 L : S ratio and stirred at ambient temperature for 2 h at a stirring rate of 250 rpm. The suspension was filtered over a Buchner, after which the leachate was boiled for 30 minutes, then filtered over a Buchner. The filtrate was stored to be used in subsequent reduction experiments.

Contaminant-metal doped (AC2) leachate. This AC2 slag is AC slag contaminated with additional heavy metal ions. It was used to test the process's tolerance to tramp metal ions. AC slag (474.05 g) was combined with Fe_2O_3 (15.00 g), MnO (5.00 g), Cr_2O_3 (1.00 g), NiO (1.40 g), SnO_2 (0.40 g) and CuO (3.15 g) and then milled in a ring mill for 30 seconds to homogenise. This mixture was then roasted in a muffle furnace for 1 h at 1200 °C, then ground in a ring mill for 5 seconds. This roasted powder was then added to 15% ammonium bicarbonate solution at an 8.33 : 1 L : S ratio and stirred at 25 °C for 2 h at a stirring rate of 250 rpm. The suspension was filtered over a Buchner, after which the leachate was boiled for 30 minutes, then filtered over a Buchner. The filtrate was stored to be used in subsequent reduction experiments.

VRC leachate. VRC slag was milled in a ring mill for 30 seconds, and then roasted in a muffle furnace under an air atmosphere for 1 h at 1000 °C. This roasted material was ground in a ring mill for 5 seconds. The powder was then added to 15% ammonium bicarbonate solution at an 8.33 : 1 L : S ratio and stirred at 50 °C for 2 h at a stirring rate of 250 rpm. The suspension was filtered over a Buchner, after which the leachate was boiled for 30 minutes, then filtered over a Buchner. The filtrate was stored to be used in subsequent reduction experiments.

Preparation of synthetic V^{5+} solution

Vanadium pentoxide (3.46 g, 19.02 mmol) was added to 15% ammonium bicarbonate solution (1 L). The solution was sonicated, boiled for 30 minutes, and then stored to be used in subsequent reduction experiments.

Reductive hydrazine precipitation

A leachate solution was added to a conical flask equipped with a magnetic stirrer bar. Hydrazine hydrate (1.5 molar equivalents relative to V, as a 10 wt% solution in water) was added, then the solution was stirred at 250 rpm and heated at 60 °C for 1 h, then 100 °C for 30 min. The suspension was allowed to cool to room

Table 1 Composition of slags determined *via* XRF. Raw slag XRF was completed on the untreated slag post-milling. Oxidised slags were oxidized in the following conditions (AC and VRC slags oxidised at 1000 °C for 1 h, AC2 slag oxidised at 1200 °C for 1 h). ND = not detected. Unroasted (raw) sample XRF values reported on a dry basis. Oxidised sample values reported on an ignited basis

	Major element analysis (wt%)														
Sample	Fe	Mn	Ti	Ca	S	P	Si	Al	Mg	V	Cu	Cr	Ni	Sn	LOI%
AC raw	15.7	2.1	2.2	36.4	ND	0.9	3.2	0.9	2.5	2.6	ND	0.3	ND	ND	
AC2 raw	18.3	3.2	1.9	33.5	ND	0.9	2.9	0.8	2.4	2.4	0.6	0.4	0.2	0.1	
VRC raw	21.5	11.5	10.0	1.6	0.1	ND	8.0	0.8	0.5	8.8	ND	ND	ND	ND	
AC ox	19.4	2.2	2.0	30.9	0.1	0.7	2.9	1.0	4.5	2.2	ND	ND	ND	ND	1.689
AC2 ox	21.3	3.2	1.9	31.7	ND	0.8	2.7	0.7	1.9	2.4	0.6	0.3	0.2	0.1	2.057
VRC ox	24.0	8.6	8.9	2.2	ND	ND	8.8	0.9	0.7	8.2	ND	ND	ND	ND	−6.438

temperature without stirring and the solids were isolated *via* centrifugation or filtration. The supernatant or filtrate was analysed *via* XRF spectrometry to determine the concentration of vanadium left in solution.

The precipitation efficiency was calculated *via* the following equation:

$$E = \left(1 - \frac{C_f}{C_i}\right) \times 100 \quad (3)$$

where E represents the precipitation efficiency expressed as a percentage, C_f is the concentration of vanadium in the solution after reduction, and C_i is the concentration of vanadium in the initial leachate solution.

Results and discussion

Proof-of-concept precipitation on a synthetic V^{5+} solution

Before investigating reductions on complex multi-metallic leachate solutions, a proof-of-concept reduction was performed on a synthetic mono-metallic solution of V^{5+} ions in 15% ammonium bicarbonate aqueous solution. Aqueous 15% bicarbonate solution was used as the solvent to be consistent with the leachate experiments described in following sections. After heating with hydrazine at 60 °C for 1 h, the colour of the solution had changed from an initial bright yellow to an extremely opaque black (Fig. 4 left and middle). The extreme opacity of this solution was suggestive of a suspension of solid particulate. The pH of this suspension was approximately 9. According to the vanadium Pourbaix diagram in water, lower-valent vanadium oxide species at this pH are solids (Fig. 2), meaning that the opaque black suspension likely is a colloid. A sample of this black suspension was slowly acidified using sulfuric acid (SI). The suspension remained an opaque black until reaching a pH of approximately 3.5, when it became a transparent dark blue/green. The colour of this solution is indicative of V^{3+} and V^{4+} ions and the transition from opaque to transparent is evidence of the dissolution of solid material. These experimental observations agree with the vanadium Pourbaix diagram in water, in which boundaries between solid and dissolved V^{3+} and V^{4+} phases lie at a pH of approximately 3.5.

Colloids are often stabilised by electrostatic interactions.[46–49] These stabilising interactions can be decreased by shifting the system towards the isoelectric point. In our ammonium bicarbonate system, this can be achieved by the removal of dissolved ammonium and carbonate ions, which are volatile and easily extracted by heating. To this end, the colloidal suspension was heated at 100 °C for 30 minutes. Successful destabilisation was evidenced by a black precipitate, which formed upon cooling the suspension to room temperature (Fig. 4 right). The solid material was collected, and the leftover leachate analysed using XRF spectrometry, which indicated a vanadium precipitation efficiency of 94%. This is comparable to efficiencies achieved in conventional ammonium-salt precipitation.[34,36,37,39]

XRD analysis of the black solid obtained after reduction and agglomeration (Fig. 5) revealed that it was a mixed valence oxide, consisting of oxides with vanadium in the V^{3+}, V^{4+}, and V^{5+} states.

TEM images of the black solid after agglomeration show clusters of cylindrical rod structures (Fig. 6a and b), which in high magnification display well defined lattice fringes (Fig. 6c and d). Surrounding the crystalline material is an approximately 5 nm thick amorphous oxide shell. These structures are uniform in size and shape, likely due to the high purity of the precipitate.

NH_4HCO_3 leaching and N_2H_4 precipitation on AC slag

After successfully isolating vanadium from a mono-metallic V^{5+} solution using a reductive hydrazine precipitation, we examined if the same process would work on a leachate from an ammonium bicarbonate leach of alkaline converter (AC) slag. This leachate contains many other contaminant ions as well as vanadium, so it is not nearly as pure and is much more comparable to real industry leachate solutions.

First, the AC slag was blank-roasted to oxidise vanadium ions in the slag to the V^{5+} state. The roasted slag was then leached in 15% ammonium bicarbonate solution at room temperature (extraction efficiency = 58%). This process was selective for vanadium and the obtained leachate composition was consistent with other literature reports of ammonium bicarbonate leaching.[25,26] The leachate was then semi-purified by boiling for 30 minutes, which removed a portion of the ammonium and carbonate ions present and resulted in the precipitation of a P–

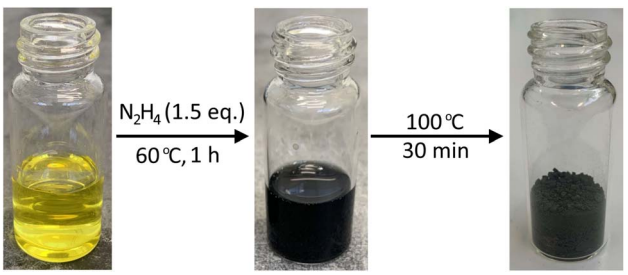

Fig. 4 Pictures of solutions and solids observed during reductive precipitation with hydrazine. Left: Initial bright yellow synthetic V^{5+} solution, middle: black colloid obtained after reduction of initial solution with hydrazine, right: black precipitate obtained after agglomeration.

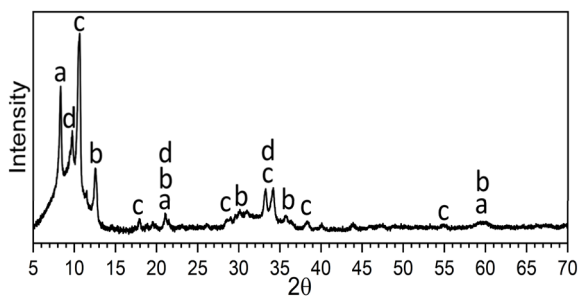

Fig. 5 XRD pattern of mixed valence vanadium oxide solid obtained after reduction of a synthetic V^{5+} solution. Labels: (a) V_4O_7, (b) $V_3O_7{\cdot}H_2O$, (c) $NH_4V_3O_7$, (d) $(NH_4)_4H_{12}V_{12}O_{36}(VO_4){\cdot}(H_2O)_{11}$.

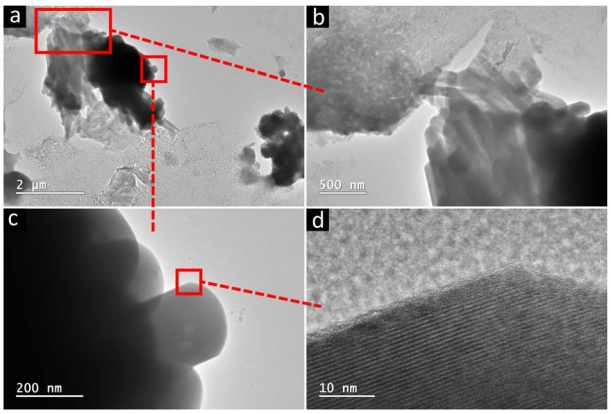

Fig. 6 TEM images of nanoparticles from a synthetic V^{5+} solution after reduction with hydrazine and agglomeration by heat. (a) Agglomerated precipitate (3k magnification), (b) stacked cylindrical rods (8k magnification), (c) rod protruding from bulk of the cluster (30k magnification), (d) the edge of a rod showing lattice fringes and an oxide shell (500k magnification).

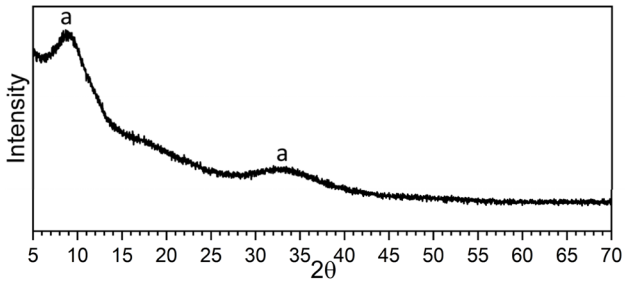

Fig. 7 XRD pattern of precipitate obtained after hydrazine precipitation on AC leachate. Labels: (a) V_4O_7.

Ca–Fe–Ti-rich byproduct, leaving a vanadium-rich leachate solution with minor amounts of phosphorus, silicon, and chromium (Table 2).

The AC leachate was then subjected to the hydrazine precipitation process. As with the mono-metallic V^{5+} solution, heating with hydrazine caused the formation of an opaque black suspension. All attempts to filter the nano-colloidal suspension without first evaporating off a portion of the dissolved organic ions were unsuccessful. However, simply heating the nano-colloid at 100 °C for 1 h formed a black precipitate which could be isolated. Agglomeration was also achieved using a flocculant (SI). The leftover solution after agglomeration by heating was analysed using XRF (AC post-agglomeration, Table 2) and compared to XRF of the initial AC leachate. This gave a precipitation efficiency of 88% (Table 2). This result is similar to hydrazine precipitation on the mono-metallic V^{5+} solution, which demonstrates that the reduction and agglomeration processes are largely unaffected by the presence of contaminant ions.

XRD analysis of this black precipitate showed the presence of a lower valent vanadium oxide, V_4O_7 (Fig. 7). The diffraction pattern obtained was broad and relatively undefined, suggesting the material is predominantly amorphous. This is in stark contrast to the sharp, well-defined peaks observed in the XRD pattern of the precipitate obtained from the proof-of-concept reduction (Fig. 5), which indicates a more crystalline phase is present in that case. The broad and diffuse peaks in the present case imply a lack of long-range order, likely due to the presence of impurities disrupting the lattice structure. No phases containing any of the impurities could be detected.

Samples of the AC precipitate before and after agglomeration were analysed using TEM. Images of the AC precipitate before agglomeration showed the presence of small vanadium-bearing nanoparticles in the range of 10–20 nm (Fig. 8a–c). In contrast, images of the precipitate after agglomeration showed large globules of particles were present, ranging in size from 100–2000 nm (Fig. 8d–f). This confirms agglomeration has occurred after heating. The agglomerated AC precipitate is considerably more undefined in structure than the precipitate obtained after reduction and agglomeration of the mono-metallic V^{5+} solution, presumably due to it being less pure. This results in largely isotropic growth with no clear ordering. These results agree with XRD analysis, which also suggested that the AC precipitate is more amorphous than the proof-of-concept precipitate.

A TEM/EDS map of the agglomerated AC precipitate showed no segregation between any of the elements present (SI).

NH_4HCO_3 leaching and N_2H_4 precipitation on other slags

Hydrazine precipitation was then tested on other leachate solutions, derived from ammonium bicarbonate leaches of VRC and AC2 slags. The VRC and AC2 slags were subjected to the

Table 2 XRF analysis of solutions before and after reduction and agglomeration, and mass of vanadium in each solution. Balance for major element analysis is H_2O. Before = leachate before hydrazine precipitation, after = leachate after hydrazine precipitation. ND = not detected. Values in brackets are the percentage precipitation efficiency of each element

		Major element analysis (mg L^{-1})						
Sample		V	Ca	Fe	Si	Cr	P	Cu
AC leachate	Before	2970	50	10	210	150	790	ND
	After	370 (88%)	10 (80%)	ND (>10%)	180 (14%)	ND (>93%)	190 (76%)	ND
VRC leachate	Before	4790	20	ND	ND	ND	ND	ND
	After	280 (94%)	ND (>50%)	ND	ND	ND	ND	ND
AC2 leachate	Before	2370	40	ND	120	230	530	10
	After	430 (82%)	10 (>75%)	ND	80 (33%)	20 (91%)	30 (94%)	ND (>10%)

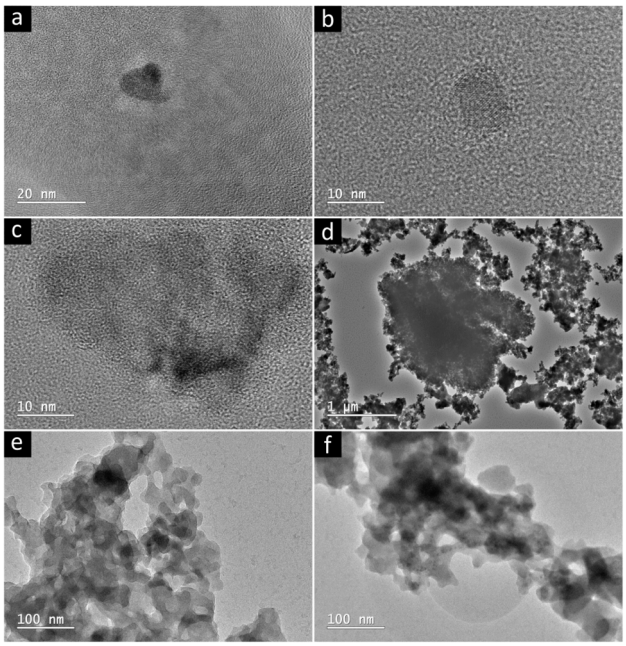

Fig. 8 TEM images of nanoparticles from AC leachate after reduction with hydrazine, before and after agglomeration by heat. (a) Individual nanoparticle before agglomeration (300k magnification), (b) individual nanoparticle before agglomeration (500k magnification), (c) nanoparticles before agglomeration (500k magnification), (d) globular cluster of nanoparticles after agglomeration (6k magnification), (e) globular cluster of nanoparticles after agglomeration (50k magnification), (f) globular cluster of nanoparticles after agglomeration (50k magnification).

same leaching procedure as the AC slag, to give two vanadium-rich leachates (Table 2). Extraction efficiencies for the ammonium bicarbonate leaches of the VRC and AC2 slags were 98% and 60%, respectively. These leachates were then run through the hydrazine precipitation process.

Hydrazine precipitation on the VRC leachate proceeded similarly to precipitations on the AC leachate and monometallic V^{5+} solution. It afforded a black powder, with a precipitation efficiency of 94% (Table 2). Hydrazine precipitation on the AC2 leachate proceeded in much the same way. The precipitation efficiency for the hydrazine process on the AC2 leachate was 82% (Table 2).

The purity and concentration of vanadium in the initial leachate solution affected the purity of the resulting vanadium-bearing oxide (Table 3 and SI). The AC precipitate was comprised of mostly vanadium oxide (>80%), with a minor amount of phosphorus oxide. Silicon, chromium, and iron oxides are also present in small quantities. The VRC leachate is much purer than the AC leachate, and, as a result, the precipitate obtained after reduction is also much purer than that of the AC version, consisting of >99.5% vanadium oxide. This level of purity is very useful in specialist applications and is highly valuable. Precipitate obtained after reduction of the AC2 leachate is the least pure, consisting of approximately 75% vanadium oxide, with phosphorus and chromium oxides making up a large portion of the impurities. The AC and AC2 precipitates could likely be purified by a second step to remove phosphorus.[34] This was, however, deemed outside the scope of this study.

Table 3 XRF analysis of vanadium-bearing oxide products obtained from hydrazine reductions of leachate solutions. ND = not detected

	Major element analysis (wt%)									
Sample	V	P	Cr	Cu	Si	Ca	Ni	Zn	Fe	Purity (%)
AC	45.5	6.7	1.1	ND	0.8	ND	ND	ND	0.1	81.2
VRC	55.7	ND	ND	ND	ND	0.2	ND	ND	0.1	99.5
AC2	42.2	8.1	2.7	0.5	0.2	0.3	0.2	0.2	ND	75.4

Regardless of which leachate is used in the reductive precipitation process, a large proportion of contaminant metal ions are also dropped out of solution after reduction and agglomeration. This leaves just a dilute aqueous solution of vanadium with trace amounts of other metal ions, which can be fully recycled to the start of the process with no detrimental effects. Significantly, chromium content in the leachate decreases dramatically after hydrazine reduction. Chromium is a common contaminant in vanadium extraction processes and is toxic and carcinogenic when in solution as the Cr^{6+} ion. After reductive precipitation with hydrazine, it is not only no longer in solution, but it is also present as a lower oxidation state which is less hazardous.

Process sustainability

Hydrazine is a strong reductant capable of reducing high-valent vanadium species to lower oxidation states at mild conditions and at ambient pressure. This reduces reagent consumption relative to conventional ammonium salt precipitation, which requires a large excess of precipitant. Importantly, hydrazine decomposes exclusively into volatile species, preventing the introduction of non-volatile contaminants into solution.

The use of ammonium bicarbonate as the lixiviant further contributes to the cleanliness of the process by eliminating the need for roasting additives, which introduce non-volatile ions into the leachate stream. As a result, the leachate is not irreversibly contaminated during the reduction and precipitation stages.

By leveraging this strategically designed reagent system, the process can operate without producing any wastewater. The leachate solution can be progressively purified *via* heating as it moves through the reduction and agglomeration processes, which results in the removal of gaseous ammonia, carbon dioxide, hydrogen, and nitrogen from the leachate, leaving just water which can be recycled to the leaching step. This represents a significant advance over traditional methods, which discharge large volumes of saline, ammoniated wastewater, thereby contributing to acid rain, smog, and eutrophication.[50,51]

Conclusions

The conventional industrial method for precipitation of vanadium from leachate solutions is detrimental to the

environment. This is primarily due to contamination of the leachate with non-volatile by-products, which necessitates the discharge of a large amount of hazardous wastewater.

We have shown that a reductive precipitation using hydrazine can generate a vanadium-bearing solid from a leachate solution, producing only clean water as a by-product. This process equals the performance of conventional methods, with precipitation efficiencies up to 94% and product purities up to 99.5% achieved. The approach works on synthetic monometallic V^{5+} solutions, as well as leachate solutions similar to those found in industry that contain contaminant metal ions.

Importantly, hydrazine doesn't leave any contaminants in solution. The oxidation of hydrazine generates only volatile by-products that can be easily separated from the leachate and captured. Combining this with ammonium bicarbonate as a lixiviant, which is also volatile, enables the leachate to be purified by simply heating. Consequently, after the process is complete, the remaining leachate solution can be recycled to the leaching step. Therefore, this is a fully zero-liquid-discharge process, outputting only solid material, whilst retaining all liquids.

The process works by utilising the difference in aqueous solubility between V^{5+} and lower valent vanadium oxides at certain pH values. Reducing in these pH windows generates solid vanadium-oxides. When hydrazine is used as the reductant, a nano-colloidal suspension of lower-valent vanadium oxides is formed, which can be agglomerated using heat to generate solid vanadium-bearing material. This concept is very versatile—it could feasibly be extended to other metal ions that have oxidation states that differ in aqueous solubility (*e.g.* Se,[52] Cu,[53] and Ru[52]), and it could potentially be 'bolted' onto the tail-end of any process that generates a vanadium-containing leachate solution.

This process significantly upgrades the vanadium content of a feed material. In cases where a leachate is contaminated with other metal ions, a solid oxide comprised mostly of vanadium is generated. This could be used in a second leach process to form pure vanadium oxides, or directly as an additive in the steel-making process.

Author contributions

AP, AM, and CB conceived the idea. AP conducted the experimental work. AP, AM, and CB analysed the data. AP, BM, AM, and CB wrote the manuscript. AP, BM, AM, and CB provided feedback on the manuscript drafts and approved the submission. CB and AM obtained the funding.

Conflicts of interest

There are no conflicts to declare.

Data availability

The data supporting this article have been included as part of the supplementary information (SI). Supplementary information: Tables S1–S5, zeta potential and particle size experiment details and results, details of flocculant ripening on nano-colloid solution, additional TEM imaging and further details of green chemistry metric calculations. See DOI: https://doi.org/10.1039/d6ra02758j.

Acknowledgements

The authors would like to thank David Flynn for their assistance with TEM imaging, and Thomas Borrmann and Chris Lepper for their assistance with zeta potential measurements and particle size analysis of the nano-colloids. This research was supported by funding received from the New Zealand Endeavour Fund, grant no.: RTVU1907.

Notes and references

1 A. A. Barani, F. Li, P. Romano, D. Ponge and D. Raabe, *Mater. Sci. Eng., A*, 2007, **463**, 138–146.
2 R. Stańko, H. Adrian and A. Adrian, *Mater. Charact.*, 2006, **56**, 340–347.
3 K. M. Eriksen, D. A. Karydis, S. Boghosian and R. Fehrmann, *J. Catal.*, 1995, **155**, 32–42.
4 R. R. Langeslay, D. M. Kaphan, C. L. Marshall, P. C. Stair, A. P. Sattelberger and M. Delferro, *Chem. Rev.*, 2019, **119**, 2128–2191.
5 M. Skyllas-Kazacos, L. Cao, M. Kazacos, N. Kausar and A. Mousa, *ChemSusChem*, 2016, **9**, 1521–1543.
6 C. Choi, S. Kim, R. Kim, Y. Choi, S. Kim, H.-y. Jung, J. H. Yang and H.-T. Kim, *Renew. Sustain. Energy Rev.*, 2017, **69**, 263–274.
7 A. Ciotola, M. Fuss, S. Colombo and W.-R. Poganietz, *J. Energy Storage*, 2021, **33**, 102094.
8 C. Brough, R. Bowell and J. Larkin, in *An Introduction to Vanadium*, ed. R. Bowell, Nova, 2019, ch. 4, pp. 87–117.
9 F. Gao, A. U. Olayiwola, B. Liu, S. Wang, H. Du, J. Li, X. Wang, D. Chen and Y. Zhang, *Miner. Process. Extr. Metall. Rev.*, 2022, **43**, 466–488.
10 K. J. Schulz, J. J. H. DeYoung, R. R. Seal II and D. C. Bradley, *Critical Mineral Resources of the United States—Economic and Environmental Geology and Prospects for Future Supply*, Report 1802, Reston, VA, 2017.
11 A. Nasimifar and J. V. Mehrabani, *International Journal of Mining and Geo-Engineering*, 2022, **56**, 361–382.
12 R. R. Moskalyk and A. M. Alfantazi, *Miner. Eng.*, 2003, **16**, 793–805.
13 C. Li, T. Jiang, J. Wen, T. Yu and F. Li, *Hydrometallurgy*, 2024, **226**, 106313.
14 R. Gilligan and A. N. Nikoloski, *Miner. Eng.*, 2020, **146**, 106106.
15 H.-Y. Li, H.-X. Fang, K. Wang, W. Zhou, Z. Yang, X.-M. Yan, W.-S. Ge, Q.-W. Li and B. Xie, *Hydrometallurgy*, 2015, **156**, 124–135.
16 J. Xiang, L. Bai, X. Lu, M. Luo, Q. Huang, S. Zhang and X. Lv, *J. Environ. Chem. Eng.*, 2023, **11**, 111304.
17 T. Chen, Y. Zhang and S. Song, *Asia-Pac. J. Chem. Eng.*, 2010, **5**, 778–784.

18 C. Li, H. Zhang, M. Tao, X. Wang, H. Li, Y. Li and Y. Tian, *Crystals*, 2021, **11**, 255.
19 M. Jung and B. Mishra, *JOM*, 2018, **70**, 168–172.
20 F. Gao, H. Du, S. Wang, B. Chen, J. Li, Y. Zhang, M. Li, B. Liu and A. U. Olayiwola, *Miner. Process. Extr. Metall. Rev.*, 2023, **44**, 352–364.
21 H.-Y. Li, C. Wang, M. Lin, Y. Guo and B. Xie, *Powder Technol.*, 2020, **360**, 503–508.
22 Y. Guo, H.-Y. Li, Y.-H. Yuan, J. Huang, J. Diao and B. Xie, *J. Hazard. Mater.*, 2020, **386**, 121948.
23 G. Du, Z. Sun, Y. Xian, H. Jing, H. Chen and D. Yin, *J. Cryst. Growth*, 2016, **441**, 117–123.
24 Y.-M. Zhang, S.-X. Bao, T. Liu, T.-J. Chen and J. Huang, *Hydrometallurgy*, 2011, **109**, 116–124.
25 M. Li, S. Zheng, B. Liu, S. Wang, D. B. Dreisinger, Y. Zhang, H. Du and Y. Zhang, *Miner. Process. Extr. Metall. Rev.*, 2017, **38**, 228–237.
26 M. Li, B. Liu, S. Zheng, S. Wang, H. Du, D. B. Dreisinger and Y. Zhang, *J. Clean. Prod.*, 2017, **149**, 206–217.
27 H.-Y. Li, J. Cheng, C.-J. Wang, S. Shen, J. Diao and B. Xie, *Metall. Mater. Trans. B*, 2022, **53**, 604–616.
28 Y. An, B. Ma, Z. Zhou, Y. Chen, C. Wang, B. Wang, M. Gao and G. Feng, *J. Environ. Chem. Eng.*, 2023, **11**, 110458.
29 H.-Y. Li, C.-J. Wang, Y.-H. Yuan, Y. Guo, J. Diao and B. Xie, *J. Clean. Prod.*, 2020, **260**, 121091.
30 H.-Y. Li, K. Wang, W.-H. Hua, Z. Yang, W. Zhou and B. Xie, *Hydrometallurgy*, 2016, **160**, 18–25.
31 M. Girdwood, A. Pearcy, T. Arif, K. Dahm, A. Marshall and C. Bumby, *ACS Sustain. Chem. Eng.*, 2025, **13**, 4376–4385.
32 Y. Muhammad and W. Lee, *Sci. Total Environ.*, 2019, **681**, 551–563.
33 M. Li, H. Du, S. Zheng, S. Wang, Y. Zhang, B. Liu, D. B. Dreisinger and Y. Zhang, *JOM*, 2017, **69**, 1970–1975.
34 P. Xiong, Y. Zhang, S. Bao and J. Huang, *Hydrometallurgy*, 2018, **180**, 113–120.
35 L. Jiang, W. He, G. Du, H. Zheng and Y. Peng, *Korean J. Chem. Eng.*, 2023, **40**, 2513–2519.
36 J. Wen, T. Jiang, W. Zhou, H. Gao and X. Xue, *Sep. Purif. Technol.*, 2019, **216**, 126–135.
37 G. Lin, J. Huang, Y. Zhang and P. Hu, *Materials*, 2022, **15**, 1945.
38 M. Gharagozlou, H. Sid Kalal, A. Khanchi, S. A. Ghorbanian, S. E. Mosavi, M. R. Almasian, D. Niknafs, A. Pourmatin and N. Akbari, *Anal. Methods Environ. Chem. J.*, 2021, **4**, 64–77.
39 B. Hu, C. Zhang, M. Yang, Q. Liu, M. Wang and X. Wang, *Hydrometallurgy*, 2021, **205**, 105742.
40 S. Liu, L. Wang, J. Chen, L. Ye and J. Du, *Sep. Purif. Technol.*, 2024, **342**, 127035.
41 S. K. Sharma, M. L. Girdwood, T. Arif, A. C. Pearcy, C. M. Tiffin, A. T. Marshall and C. W. Bumby, *Hydrometallurgy*, 2025, **232**, 106433.
42 A. Furst, R. C. Berlo and S. Hooton, *Chem. Rev.*, 1965, **65**, 51–68.
43 G. Byrkit and G. Michalek, *Ind. Eng. Chem.*, 1950, **42**, 1862–1875.
44 M. Vogel, A. Büldt and U. Karst, *Fresenius. J. Anal. Chem.*, 2000, **366**, 781–791.
45 B. T. Heaton, C. Jacob and P. Page, *Coord. Chem. Rev.*, 1996, **154**, 193–229.
46 O. Z. Sharaf, R. A. Taylor and E. Abu-Nada, *Phys. Rep.*, 2020, **867**, 1–84.
47 D. J. Pochapski, C. Carvalho dos Santos, G. W. Leite, S. H. Pulcinelli and C. V. Santilli, *Langmuir*, 2021, **37**, 13379–13389.
48 J. Hierrezuelo, A. Sadeghpour, I. Szilagyi, A. Vaccaro and M. Borkovec, *Langmuir*, 2010, **26**, 15109–15111.
49 S. H. Behrens, D. I. Christl, R. Emmerzael, P. Schurtenberger and M. Borkovec, *Langmuir*, 2000, **16**, 2566–2575.
50 L. Guo, Y. Xie, W. Sun, Y. Xu and Y. Sun, *Water*, 2023, **15**, 684.
51 H. Vo, H. Ngo, W. Guo, S. Chang, D. Nguyen, Z. Chen, X. Wang, R. Chen and X. Zhang, *Crit. Rev. Environ. Sci. Technol.*, 2020, **50**, 1224.
52 Z. Wang, X. Guo, J. Montoya and J. K. Nørskov, *npj Comput. Mater.*, 2020, **6**, 160.
53 B. Beverskog and I. Puigdomenech, *J. Electrochem. Soc.*, 1997, **144**, 3476.